Inorganic Chemistry

Article

pubs.acs.org/IC

# Host Sensitization of $Tb^{3+}$ Ions in Tribarium Lanthanide Borates $Ba_3Ln(BO_3)_3$ (Ln = Lu and Gd)

De-Yin Wang,[†] Teng-Ming Chen,*[,†] and Bing-Ming Cheng[‡]

[†]Phosphors Research Laboratory and Department of Applied Chemistry, National Chiao Tung University, Hsinchu 30010, Taiwan

[‡]National Synchrotron Radiation Research Center (NSRRC), Hsinchu 30076, Taiwan

**ABSTRACT:** The vacuum-ultraviolet (VUV) spectroscopic properties of undoped and $Tb^{3+}$-doped borates $Ba_3Ln(BO_3)_3$ (Ln = Lu and Gd) with different crystal structures were investigated by using synchrotron radiation. $Ba_3Lu(BO_3)_3$ (BLB) crystallizes in a hexagonal structure, whereas $Ba_3Gd(BO_3)_3$ (BGB) crystallizes in a trigonal structure. The maximum host absorption for BLB and BGB was found to locate at ~179 and ~195 nm, respectively. Upon host excitation, BLB exhibits an intrinsic broad UV emission centered at 339 nm, which is attributed to the recombination of self-trapped excitons that may presumably be associated with band-gap excitations or molecular transitions within the $BO_3^{3-}$ group. In contrast to BLB, no broad emission but line emission ascribed to a $Gd^{3+}$ $^6P_J$–$^8S_{7/2}$ transition was observed in the emission spectrum of BGB. Upon doping of $Tb^{3+}$ ions into the hosts of BLB and BGB, an efficient energy transfer from the host excitations to $Tb^{3+}$ via host/$Gd^{3+}$ emission was observed, showing that host sensitization of $Tb^{3+}$ occurs in these rare-earth borates.

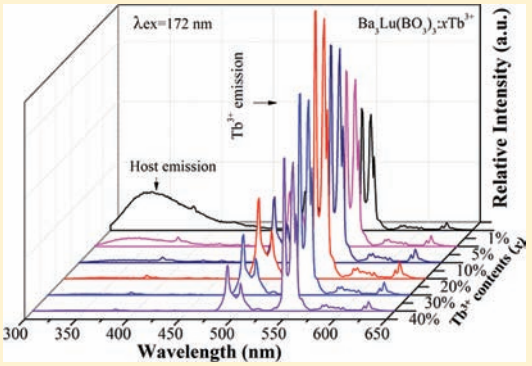


## INTRODUCTION

Because of theoretical interests and industrial demand for efficient vacuum-ultraviolet (VUV) excited phosphors for mercury-free fluorescent lamps and plasma display panels (PDPs), in which the VUV radiation from a noble gas discharge is used as the excitation source for phosphors, growing attention has been paid to the luminescence spectroscopy of rare-earth ions in the VUV spectral region (wavelength $\lambda$ < 200 nm; energy $E$ > 50 000 $cm^{-1}$) during the past few years.[1−12] The problem here is that the excitation process of a phosphor under VUV excitation is very different from that under ultraviolet excitation because of the energy difference; consequently, a good phosphor for ultraviolet excitation (e.g., used in a fluorescent lamp) is certainly not a good choice for VUV excitation. Thus, in the field of PDPs, it is necessary to develop new phosphors that could efficiently convert VUV light into visible light. Upon VUV excitation, it is considered that most of the incident photons are absorbed by the host crystal moving electrons from the valence band toward the conduction band, subsequently producing either self-trapped excitons (STEs) or free electron−hole pairs.[13] If the STE emission overlaps absorption of the activator, then resonant energy from the host to activator could occur according to the Forster−Dexter theory, giving rise to an efficient luminescence from the activator in such a host. On the other hand, most phosphors currently used in PDPs show strong emission under VUV excitation, but they still have some insufficiencies; for example, the commonly used green-emitting phosphor $Zn_2SiO_4$:$Mn^{2+}$ has a relative long decay time, which will cause image delay in the case of rapid-moving pictures.[14] To solve this problem, one alternative approach is to develop new phosphor materials with higher VUV absorption and shorter decay time. Tribarium lanthanide borates $Ba_3Ln(BO_3)_3$ (Ln = La−Lu and Y) are of particular interest for us because some isostructural compounds of this family have been shown to exhibit intrinsic host emission when excited by X-ray radiation.[15] Similar to X-ray radiation, VUV radiation also has high energy; therefore, in the case of VUV excitation, the same host emission from these compounds is expected. In addition, $Tb^{3+}$ is a well-known green-emitting ion. If $Tb^{3+}$ ions are introduced into these borate compounds, host sensitization of $Tb^{3+}$ ions would occur. This paper is devoted to studying the VUV-excited luminescence of $Ba_3Ln(BO_3)_3$ (Ln = Lu and Gd) and energy transfer from the host excitation to the doped $Tb^{3+}$ ions.

## EXPERIMENTAL SECTION

**Materials and Synthesis.** Powder samples of $Tb^{3+}$-doped and undoped $Ba_3Lu(BO_3)_3$ (BLB) and $Ba_3Gd(BO_3)_3$ (BGB) were synthesized by high-temperature solid-state reaction. $BaCO_3$ (99.9%, Sigma-Aldrich), $H_3BO_3$ (99.99%, Sigma-Aldrich), $Lu_2O_3$ (99.99%, Grirem), $Gd_2O_3$ (99.99%, Grirem), and $Tb_4O_7$ (99.9%, Aldrich) were used as reagents. The oxides were mixed according to the desired stoichiometric ratios of each sample and then were thoroughly ground. The obtained mixtures were fired at 1100 °C in a reducing atmosphere (15% $H_2$/85% Ar) for the $Tb^{3+}$-doped samples and in air for the undoped samples.

**Characterization Methods.** The phase purity of all samples was checked by using powder X-ray diffraction (XRD) analysis with a

**Received:** October 16, 2011
**Published:** February 23, 2012

 © 2012 American Chemical Society  dx.doi.org/10.1021/ic202241h | *Inorg. Chem.* 2012, 51, 2961−2965

Bruker AXS D8 advanced automatic diffractometer operated at 40 kV and 40 mA with Cu K$\alpha$ radiation ($\lambda$ = 1.5418 Å).

The VUV photoluminescence (PL) spectra were recorded at the Beamline 03A at the NSRRC in Taiwan. The experimental setup for the PL spectra was similar to that described elsewhere.[16] In summary, VUV excitation light from the high-flux beamline attached to the 1.5-GeV storage ring was dispersed with a 6-m cylindrical-grating monochromator (CGM). The intensity of the VUV light was monitored with a gold mesh transmitting about 90% and recorded with an electrometer (Keithley 6512). The VUV synchrotron light transmitted through the gold mesh irradiated the sample, which was arranged at angles near 45° with respect to both the incident VUV source and the entrance slit of the dispersing monochromator. A Jobin-Yvon HR320 instrument equipped with a 1200 lines/mm grating and a Hamamatsu R943-02 photomultiplier tube was used to record the PL spectra. For measurement of the PL excitation (PLE) spectra, the dispersive emission was monitored at a selected band, in which the CGM beamline with a 450 lines/mm grating was scanned. All of the PLE spectra were normalized with the spectral response curve of the CGM beamline.

## RESULTS AND DISCUSSION

**Crystal Structure and Phase Identification.** Although BLB and BGB have similar compositions, they crystallize in different crystal structures. Parts a and b of Figure 1 present the

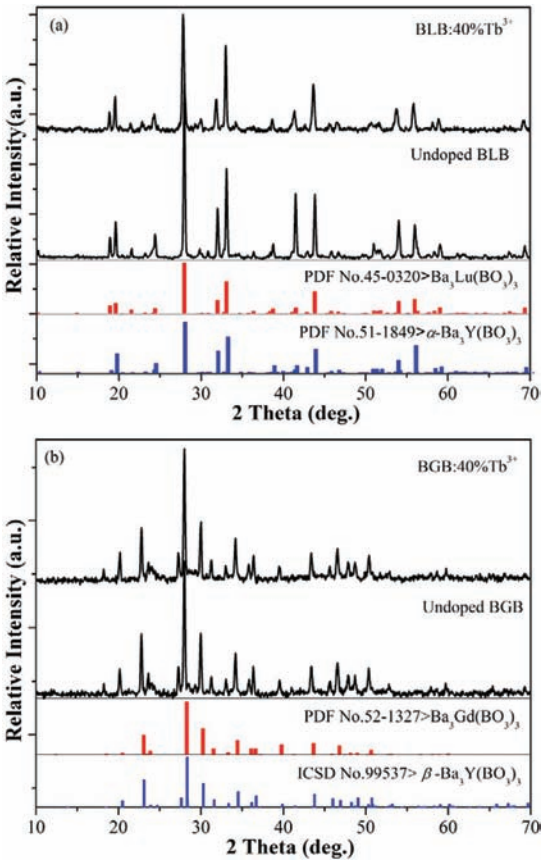


**Figure 1.** XRD patterns of undoped and 40% $Tb^{3+}$-doped BLB and BGB as well as PDF cards 45-0320 of BLB, 51-1849 of $\alpha$-$Ba_3Y(BO_3)_3$, and 52-1327 of BGB and ICSD card 99537 of $\beta$-$Ba_3Y(BO_3)_3$.

XRD patterns of the undoped and 40% $Tb^{3+}$-doped BLB and BGB. All samples are identified as single phase by using the reported standard XRD patterns of BLB (PDF no. 45-0320) and BGB (PDF no. 52-1327) as references. Detailed crystal structures of BLB and BGB have not been reported so far; however, the crystal structure of their isostructral compound $Ba_3Y(BO_3)_3$ has been well studied.[17−19] From refs 17−19, it is known that $Ba_3Y(BO_3)_3$ crystallizes in a low-temperature phase [$\alpha$-$Ba_3Y(BO_3)_3$] with a hexagonal system ($P6_3cm$, $Z$ = 6) or a high-temperature phase [$\beta$-$Ba_3Y(BO_3)_3$] with a trigonal system ($R\bar{3}$, $Z$ = 6), depending on the calcination temperature.[17−19] The crystal structure of $\alpha$-$Ba_3Y(BO_3)_3$ consists of isolated $BO_3$ triangles with Y−O octahedra and Ba−O polyhedra,[17,18] while that of $\beta$-$Ba_3Y(BO_3)_3$ is built from a $YB_6O_{18}$ unit with polyhedra of $BaO_6$ and $BaO_8$.[19] In both phases, Y atoms are six-coordinated.[17−19] The big difference between the two phases is that there are $BO_3$ triangle layers in the structure of $\alpha$-$Ba_3Y(BO_3)_3$, which do not exist in that of $\beta$-$Ba_3Y(BO_3)_3$.[17−19] The XRD patterns of undoped and $Tb^{3+}$-doped BLB are analogous to that of $\alpha$-$Ba_3Y(BO_3)_3$ (PDF no. 51-1849; see Figure 1), suggesting that both undoped and $Tb^{3+}$-doped BLB crystallize in an $\alpha$-$Ba_3Y(BO_3)_3$-related structure. However, as indicated in Figure 1b, the XRD patterns of undoped and $Tb^{3+}$-doped BGB differ from that of $\alpha$-$Ba_3Y(BO_3)_3$ and resemble that of $\beta$-$Ba_3Y(BO_3)_3$ (ICSD no. 99537), indicating that both undoped and $Tb^{3+}$-doped BGB crystallize in a $\beta$-$Ba_3Y(BO_3)_3$-related structure.

**VUV Spectroscopy of BLB and BLB:$Tb^{3+}$.** The PL and PLE spectra of undoped BLB are shown in Figure 2. Upon host

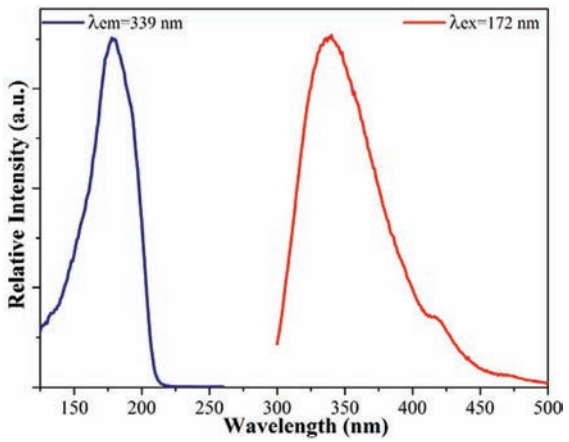


**Figure 2.** PLE and PL spectra of undoped BLB obtained by monitoring the STE emission at 339 nm and under excitation at 172 nm.

excitation at 172 nm, BLB emits a broad intrinsic UV-luminescence band with a maximum at 339 nm and a half-width of about 6020 $cm^{-1}$. The emission band most likely arises from the recombination of STEs that may be associated with band-gap excitations or molecular transitions within the $BO_3^{3-}$ group.[20,21] By monitoring the intrinsic UV emission at 339 nm, the PLE spectrum of BLB was obtained. The broad excitation band with a maximum at round 179 nm could be associated with band-gap excitations or molecular transitions within the $BO_3^{3-}$ group.[20] The tail of the intrinsic UV emission partially overlaps with the $Tb^{3+}$ 4f−4f absorptions (e.g., $^7F_6$−$^5D_3$ absorption), providing conditions for Forster−Dexter energy transfer. Thus, when $Tb^{3+}$ ions are introduced to the host lattice of BLB, an efficient energy transfer from host excitation to $Tb^{3+}$ ions is expected. To confirm this expectation, the PL spectra of BLB containing different concentrations of $Tb^{3+}$ were measured and shown in Figure 3. With increasing $Tb^{3+}$ doping concentration, the increase of $Tb^{3+}$ emission from


dx.doi.org/10.1021/ic202241h | Inorg. Chem. 2012, 51, 2961−2965

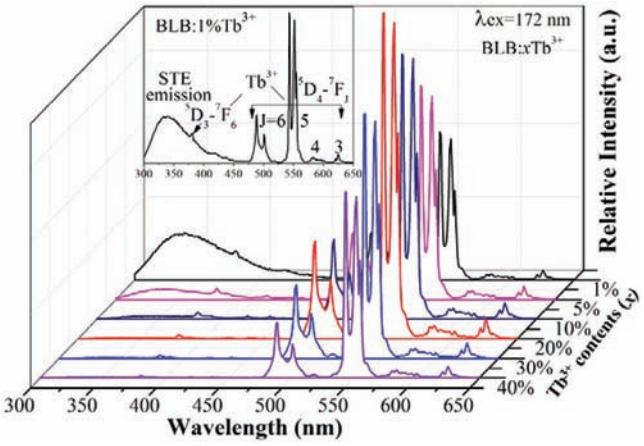


**Figure 3.** PL spectra of BLB:$x$Tb$^{3+}$ (1% ≤ $x$ ≤ 40%) excited at 172 nm. The inset shows the assigned PL spectrum of BLB:1% Tb$^{3+}$.

its $^5D_4$ level is accompanied by the significant reduction of STE emission, giving a strong evidence to the occurrence of STE-to-Tb$^{3+}$ energy transfer. A weak $^5D_3$–$^7F_6$ transition of Tb$^{3+}$ around 380 nm can be observed in the PL spectra of BLB:$x$Tb$^{3+}$ at low Tb$^{3+}$ doping concentration (<10%), implying that energy transfer from STE to Tb$^{3+}$ involves the Tb$^{3+}$ $^5D_3$ state. When increasing Tb$^{3+}$ concentration up to 10%, STE emission was almost quenched because of energy transfer, and with further increasing Tb$^{3+}$ concentration to 20%, the emission originating from the Tb$^{3+}$ $^5D_4$ state starts to decrease because of the concentration quenching effect. To give further evidence to support the occurrence of host-to-Tb$^{3+}$ energy transfer, the PLE spectrum of BLB:5% Tb$^{3+}$ obtained by monitoring the Tb$^{3+}$ emission at 543 nm was measured, and a comparison was made with that of the undoped BLB (see Figure 4). The two

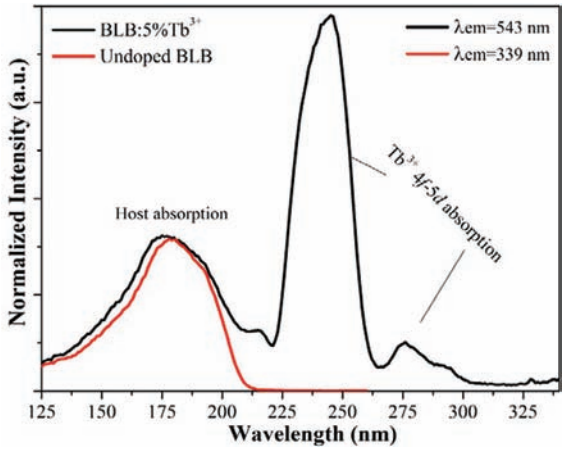


**Figure 4.** PLE spectra of 5% Tb$^{3+}$-doped BLB monitoring Tb$^{3+}$ emission at 543 nm and undoped BLB monitoring the STE emission at 339 nm. The PLE spectra are normalized on the host absorption intensity.

PLE spectra exhibit general features similar to those of a broad band below 210 nm, indicating that they both result from the same origin. As indicated in Figure 4, the presence of the host absorption band in the PLE spectrum of 5% Tb$^{3+}$-doped BLB, monitored within the Tb$^{3+}$ emission, further supports that energy transfer from the host to Tb$^{3+}$ really occurred. Furthermore, the strong excitation bands in the region from 210 to 300 nm are assigned to the interconfiguration 4f$^8$–4f$^7$5d$^1$ transition of Tb$^{3+}$. When one electron of Tb$^{3+}$ is promoted from the ground state with a 4f$^8$ configuration to the excited state with a 4f$^7$5d$^1$ configuration, it will produce a more energetic spin-allowed 4f$^8$–4f$^7$5d$^1$ transition and a less energetic spin-forbidden 4f$^8$–4f$^7$5d$^1$ transition.[5] Therefore, it is considered that the strong excitation band centered at 243 nm is from a Tb$^{3+}$ spin-allowed 4f$^8$–4f$^7$5d$^1$ transition, while the weak band at 275 nm is from a spin-forbidden transition. In addition, BLB has a XRD pattern similar to that of $Ba_3Sc(BO_3)_3$ (see ICSD no. 75340), suggesting that they have the same crystal structure. A preliminary structural study of $Ba_3Sc(BO_3)_3$ has shown that there are two crystallographically independent types of Sc atoms occupying the distorted octahedral sites having $C_3$ and $C_{3v}$ point symmetries,[22] which is considered to be the same case for BLB. The low symmetry of the Tb$^{3+}$ site in BLB:Tb$^{3+}$ would result in the splitting of the Tb$^{3+}$ 5d orbital, the contribution of which to the origin of the shoulder at 275 nm cannot be excluded. The strong quenching of host emission (or STE emission) and the increased PL intensity of Tb$^{3+}$ emission with increasing of Tb$^{3+}$ dopant concentrations along with a similar host absorption band for both undoped and Tb$^{3+}$-doped BLB suggest that an efficient energy transfer from the host excitations to Tb$^{3+}$ occurs in BLB:$x$Tb$^{3+}$ phosphors.

**VUV Spectroscopy of BGB and BGB:Tb$^{3+}$.** As indicated by the PL and PLE spectra of BGB in Figure 5, the PLE

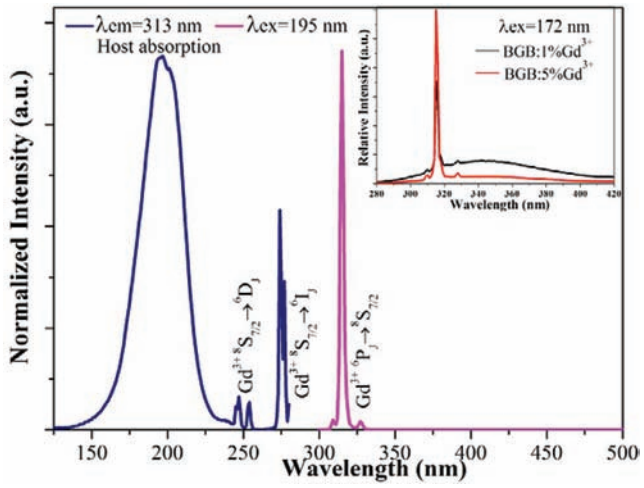


**Figure 5.** PLE and PL spectra of undoped BGB obtained by monitoring the Gd$^{3+}$$^6P_J$–$^8S_{7/2}$ emission at 313 nm and under excitation at 195 nm. The inset shows the PL spectra of 1% and 5% Gd$^{3+}$-doped BLB excited at 172 nm.

spectrum of BGB is dominated by a broad host absorption band with a maximum at about 195 nm, and sharp-line absorptions at 254 and 273 nm were assigned to the intraconfigurational 4f–4f excitation from the $^8S_{7/2}$ ground state to the $^6D_J$ and $^6I_J$ excited states of Gd$^{3+}$, respectively.[3] Comparing the PLE spectrum of BGB with that of BLB, we have found that the host absorption maximum of BGB (~195 nm) located at a longer-wavelength side than that of BLB (~179 nm), suggesting that the band gap of BGB is narrower than that of BLB. Upon host excitation at 195 nm, instead of the intrinsic broad UV emission band observed in the PL spectrum of BLB, only a sharp-line emission at 313 nm ascribed to the Gd$^{3+}$ $^6P_J$–$^8S_{7/2}$ transition was observed in the PL spectrum of BGB. However, it is considered that the molecular


dx.doi.org/10.1021/ic202241h | Inorg. Chem. 2012, 51, 2961–2965

transitions within the $BO_3^{3-}$ group in BGB would also give rise to the same STE emission as that in BLB, and because of energy transfer from the STE emission to $Gd^{3+}$ ions, the expected STE emission was quenched and not observed in the PL spectrum of BGB. To give evidence to support this deduction, we have measured the PL spectra of the BLB phosphors containing 1% and 5% $Gd^{3+}$, respectively, and presented the results in the inset of Figure 5. We have observed that when a small amount of the $Gd^{3+}$ ion is introduced into the host lattice of BLB, the PL intensity of the host emission greatly decreased with the appearance of the emission originating from the $Gd^{3+}$ $^6P_J$ level. This replacement of the STE emission with the $Gd^{3+}$ $^6P$ emission clearly confirms the energy transfer from STE to $Gd^{3+}$.

Shown in Figure 6 are the PL spectra of BGB:$x$Tb$^{3+}$ ($0 \le x \le$ 40%) excited at 195 nm. The PL spectra of BGB:$x$Tb$^{3+}$ ($0 \le x$

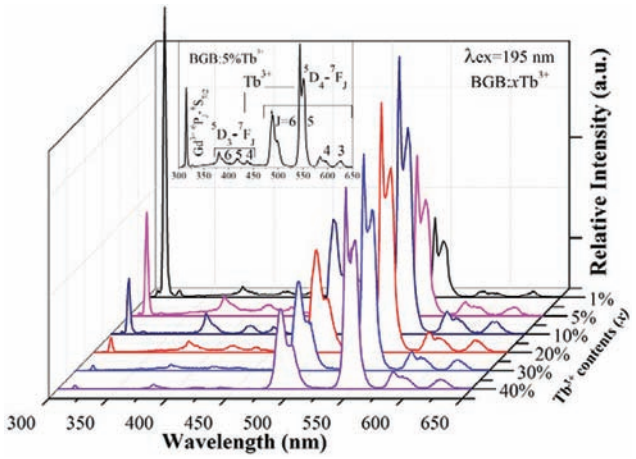


**Figure 6.** PL spectra of BGB:$x$Tb$^{3+}$ ($1\% \le x \le 40\%$) excited at 195 nm. The inset shows the assigned PL spectrum of BGB:5% Tb$^{3+}$.

$\le$ 40%) are composed of emissions originating from the $Gd^{3+}$ $^6P_J$ level at 313 nm and the $Tb^{3+}$ $^5D_3$ and $^5D_4$ levels in the 365–470 and 470–650 nm regions, respectively. For BGB:$x$Tb$^{3+}$ samples with low $Tb^{3+}$ doping concentration (e.g., $x$ = 1%), the observed PL spectrum is dominated by the $Gd^{3+}$ emission. However, with increasing $Tb^{3+}$ dopant concentration, the emission intensity from the $Tb^{3+}$ $^5D_4$ level increases and the PL spectra become dominated by the $Tb^{3+}$ $^5D_4$ emission. With further increasing $Tb^{3+}$ dopant concentration ($x$ > 10%), the $Tb^{3+}$ emission intensity begins to decease because of the concentration quenching effect. In the meantime, the intensity of the $Gd^{3+}$ emission decreases significantly because of $Gd^{3+} \rightarrow Tb^{3+}$ energy transfer. It is worth mentioning here that the emission spectrum of $Tb^{3+}$ in BLB is slightly different from that in BGB. Specifically, the $Tb^{3+}$ $^5D_4$–$^7F_5$ emission splits roughly into three peaks in BLB, while it splits into two peaks in BGB. Because BGB has a XRD pattern tsimilar o that of $Sr_3Sc(BO_3)_3$ (refer to ICSD no.75339), which implies that they have similar crystal structures. There are two nonequivalent Sc sites in $Sr_3Sc(BO_3)_3$, and both Sc atoms occupy distorted octahedral sites having $S_6$ point-group symmetry.[23] Therefore, it is considered that $Tb^{3+}$ in BGB:$Tb^{3+}$ also has $S_6$ symmetry. As mentioned previously in section 3.2, the $Tb^{3+}$ ions in BLB:$Tb^{3+}$ possess $C_3$ and $C_{3v}$ symmetry, respectively. Therefore, the different local environments for $Tb^{3+}$ in BGB and BLB may lead to a different splitting of the $Tb^{3+}$ emission, which accounts for the observed different $Tb^{3+}$ emission spectra. As shown in Figure 7, the PLE spectrum of BGB:5% $Tb^{3+}$,

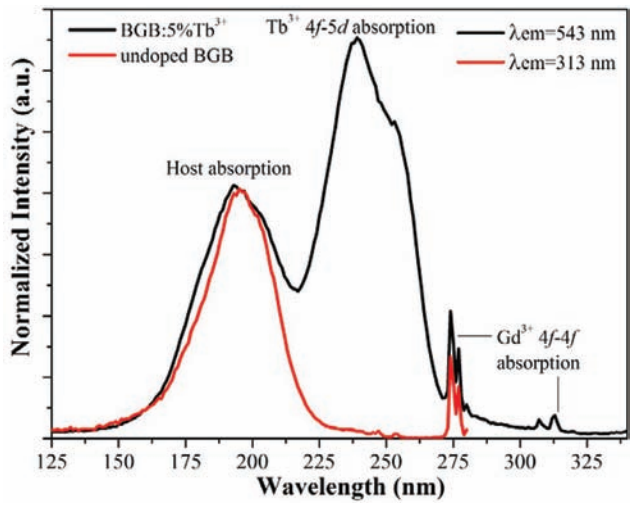


**Figure 7.** PLE spectra of 5% $Tb^{3+}$-doped BGB monitoring the $Tb^{3+}$ emission at 543 nm and undoped BGB monitoring the $Gd^{3+}$ emission at 313 nm. The PLE spectra are normalized on the host absorption intensity.

obtained by monitoring the emission from the $Tb^{3+}$ $^5D_4$ level at 543 nm, is found to consist of host absorption in the 125–225 nm region, the $Tb^{3+}$ 4f–5d absorption in the 225–300 nm region, and $Gd^{3+}$ 4f–4f absorption at around 273 nm. Except the $Tb^{3+}$ 4f–5d absorption band, the PLE spectrum of the BGB:5% $Tb^{3+}$ sample is almost identical with that of the undoped BGB, which further confirms that the absorption band in the 125–225 nm range originated from host absorption. The observation that the intensity of the $Gd^{3+}$ $^6P_J$–$^8S_{7/2}$ emission decreases with increasing $Tb^{3+}$ concentration together with the presence of host and $Gd^{3+}$ absorption in the PLE spectrum, obtained by monitoring the $Tb^{3+}$ emission of BGB:5% $Tb^{3+}$, provides clear evidence for the host–$Gd^{3+}$–$Tb^{3+}$ energy transfer.

## CONCLUSIONS

In summary, we have investigated the VUV-excited luminescence of undoped and $Tb^{3+}$-doped $Ba_3Ln(BO_3)_3$ (Ln = Lu and Gd) phosphors with two different crystal structures. BLB has a low-temperature-phase $\alpha$-$Ba_3Y(BO_3)_3$-related structure, while BGB has a high-temperature-phase $\beta$-$Ba_3Y(BO_3)_3$-related structure. The PLE spectra reveal that the band gap of BLB (~179 nm) is broader than that of BGB (~195 nm). Upon host excitation, the emission spectrum of BLB is composed of a broad UV emission that is attributed to the recombination of STEs, whereas the emission spectrum of BGB is dominated by line emission originating from the $Gd^{3+}$ $^6P_J$–$^8S_{7/2}$ transition, which is the result of host-to-$Gd^{3+}$ energy transfer via STE emission. When $Tb^{3+}$ ions are incorporated into BLB and BGB, efficient energy transfer from the host excitations to $Tb^{3+}$ via STE or $Gd^{3+}$ emission was observed. The strong quenching of the host/$Gd^{3+}$ emission and similar excitation spectra of the $Tb^{3+}$-doped and undoped samples give conclusive evidence for such an energy transfer.


dx.doi.org/10.1021/ic202241h | Inorg. Chem. 2012, 51, 2961–2965

## AUTHOR INFORMATION

### Corresponding Author

*E-mail: tmchen@mail.nctu.edu.tw. Tel: + 886-35731695. Fax: + 886-35723764.

### Notes

The authors declare no competing financial interest.

## ACKNOWLEDGMENTS

We gratefully thank the National Science Council of Taiwan for financial support under Contracts NSC99-2811-M-009-052 (D.-Y.W.) and NSC98-2113-M-009-005-MY3 (T.-M.C.).

## REFERENCES

(1) Wegh, R. T.; Donker, H.; Holsa, J.; Meijerink, A. *Phys. Rev. B* **1997**, *56*, 13841−13848.
(2) Zhou, Y.; Feofiov, S. P.; Seo, H. J.; Jeong, J. Y.; Keszler, D. A.; Meltzer, R. S. *Phys. Rev. B* **2008**, *77*, 075129−075133.
(3) Wegh, R. T.; Donker, H.; Oskam, K. D.; Meijerink, A. *Science* **1999**, *283*, 663−666.
(4) Wegh, R.; Vanloef, E.; Meijerink, A. *J. Lumin.* **2000**, *90*, 111−122.
(5) Wang, D. Y.; Kodama, N.; Zhao, L. *J. Electrochem. Soc.* **2010**, *157*, J233−J237.
(6) Beauzamy, L.; Moine, B.; Meltzer, R. S.; Zhou, Y.; Kim, K. J.; Gredin, P. *Phys. Rev. B* **2008**, *78*, 184302−184312.
(7) Tian, Z. F.; Liang, H. B.; Chen, W. P.; Su, Q.; Zhang, G. B.; Yang, G. T. *Opt. Express.* **2009**, *17*, 956−962.
(8) Kubota, S.; Shimada, M. *Appl. Phys. Lett.* **2002**, *81*, 2749−2751.
(9) Im, W. B.; Kang, J. H.; Lee, D. C.; Lee, S.; Jeon, D. Y.; Kang, Y. C.; Jung, K. Y. *Solid State Commun.* **2005**, *133*, 197−201.
(10) Jung, I. Y.; Cho, Y.; Lee, S. G.; Sohn, S. H.; Kim, D. K.; Lee, D. K.; Kweon, Y. M. *Appl. Phys. Lett.* **2005**, *87*, 191908−191910.
(11) Im, W. B.; Kim, Y.; Yoo, H. S.; Jeon, D. Y. *Inorg. Chem.* **2009**, *48*, 557−564.
(12) Xie, M. B.; Tao, Y.; Huang, Y.; Liang, H. B.; Su, Q. *Inorg. Chem.* **2010**, *49*, 11317−11324.
(13) Moine, B.; Bizarri, G. *Opt. Mater.* **2006**, *28*, 58−63.
(14) Morell, A.; Khiati, N. E. *J. Electrochem. Soc.* **1993**, *140*, 2019−2022.
(15) Duan, C. J.; Yuan, J. L.; Zhao, J. T. *J. Solid State Chem.* **2005**, *178*, 3698−3702.
(16) Lu, H. C.; Cheng, B. M. *Anal. Chem.* **2011**, *83*, 6539−6544.
(17) Khamaganova, T. N.; Kuperman, N. M.; Bazarova, Z. G. *J. Solid State Chem.* **1999**, *145*, 33−36.
(18) Li, X. Z.; Chen, X. L.; Wu, L.; Cao, Y. G.; Zhou, T.; Xu, Y. P. *J. Alloys Compd.* **2004**, *370*, 53−58.
(19) Li, X. Z.; Chen, X. L.; Jian, J. K.; Wu, L.; Xu, Y. P.; Cao, Y. G. *J. Solid State Chem.* **2004**, *177*, 216−220.
(20) Feofilov, S. P.; Zhou, Y.; Jeong, J. Y.; Keszler, D. A.; Meltzer, R. S. *J. Lumin.* **2007**, *125*, 80−84.
(21) Ogorodnikov, I. N.; Pustovarov, V. A.; Kruzhalov, A. V.; Isaenko, L. I.; Kirm, M.; Zimmerer, G. *Phys. Solid State* **2000**, *42*, 454−462.
(22) Cox, J. R.; Keszler, D. A.; Huang, J. F. *Chem. Mater.* **1994**, *6*, 2008−2013.
(23) Thompson, P. D.; Keszler, D. A. *Chem. Mater.* **1994**, *6*, 2005−2007.